



# Comparison between negative velocity feedback control and time delay velocity control of a nonlinear beam

H. Mosaa<sup>1\*</sup>, M. Kamel<sup>2</sup>, H. El – Gohary<sup>2</sup>, L. S. Diab<sup>1</sup>, H. M. Shawky<sup>1</sup>

<sup>1</sup> Department of Mathematics, Faculty of Science(Girls Branch) , AL-Azhar University, Egypt

<sup>2</sup> Department of Engineering Mathematics, Faculty of Electronic Engineering, Menofia University, Egypt

\* E-mail address:[heba.elsayed@azhar.edu.eg](mailto:heba.elsayed@azhar.edu.eg)

## Abstract

In that work, vibrations for the nonlinear beam under harmonic external forcing are investigated and studied. Vibration control is discussed by using both the negative velocity feedback and the time delay. The multiple scale perturbation technique (MSPT) is utilized to study the approximate solutions for the given beam system. Stability investigations are studied close to the primary resonance case ( $\Omega \cong \omega_1$ ) to reach the frequency response equations (FRE). The beam system's time history figures and various response curves prior to and after control are investigated numerically. Numerical results of the effects of various parameters illustrated the best conditions for reducing the vibration. The obtained results demonstrated that the negative velocity feedback control's efficiency is superior to the time delay control. Lastly, the solution of analytical and numerical accord well with one another.

7796

**Key words:** Nonlinear beam, vibration control, feedback control, stability, time delay

**DOI Number:**10.14704/nq.2022.20.8.NQ44804

**NeuroQuantology 2022; 20(8): 7796-7809**

## 1. Introduction

One of the more thrilling subjects in the area of physics is chaos. For this reason, many scholars from different domains dedicated a lot of effort for analyzing chaotic demeanor besides controlling oscillations and chaos to different shaking systems. Over the past 20 years, numerous concepts and techniques for dominating chaos have been suggested [1–5]. Additionally, vibrations are undesirable phenomenon because they are the cause of damage, noise and occasionally destroy the entire systems, which represent in a lot of engineering applications like machinery and beam structures. Eissa and Sayed [6] discussed the various proceedings linked to the vibration experiment for a system of engineering besides the essential concepts and vibration connotations. However, techniques such as

passive and active control have been utilized in machinery and structures for reducing oscillations and dynamics of chaos.

Utilizing a piezoelectric substance, Li et al. [7] investigated the nonlinear elastic beam's vibration under harmonic external force. The nonlinear equation describing the beam's motion was derived by employing Hamilton's principle. Additionally, for solving the cubic nonlinear equation of motion together with the damping coefficient, the perturbation method is utilized to get the approximation of the first order. They found that the control of velocity feedback is utilized to improve the unsteady resonance, as well as the outer control voltages supplied to the piezoelectric actuators, which are applied to illustrate the viability of the active control approach. Yaman and Sen [8] applied the control of negative cubic velocity



feedback to put down the vibrations of a cantilever beam that has varying directions under the effect of a mix of external and parametric excitation forces. The amplitude-frequency relation and phases are got by utilizing the perturbation approach, and the impacts of the system's parameters are discussed using numerical techniques. Also, Hegazy [9] discussed the phenomenon of saturation and nonlinear vibrations within the controlled hinged-hinged elastic beam. When different control strategies were compared for effectiveness, it was discovered that negative velocity feedback was the most effective way to suppress oscillations in the system. Moreover, in Hegazy [10] implemented a number of controllers for reducing the vibrations and chaotic behaviors of the beam's first mode at primary resonance caused by the effect of external and parametric forces. Applying the multiple scales technique in order to get the analytical solutions of the beam. According to their results, the linear position feedback controller (LPF) performs the best among positive position feedback controllers, whereas among velocity feedback controllers the cubic velocity feedback (CVF) control is the best.

The approach of time-delayed control is a new method for suppressing vibration.

As a result, numerous researchers have developed a lot of studies on the control of systems using time delay control. Maccari [11,12] applied the time delay control for the systems of Lienard of a Van der Pol-Duffing oscillator. Utilizing the perturbation approach to get the motion's equations and phases. From the standpoint of vibration control for suppressing the system's oscillation, the best options of feedback gains and time delay are found. Also, it is proved that stable cyclic solutions with arbitrarily chosen amplitudes can be achieved if terms of the vibration control are added. As a result, the outcomes shown that the efficient control of the vibration amplitude is feasible if the selection of adequate time delay and gains of the feedback. El-Ganaini and El-Gohary [13,14] applied the time delay absorber control for reducing the messy vibrations of the nonlinear oscillating

system under the effect of multi-external and multi-parametric forces. The Rung-Kutta fourth order approach and (FRE) equation are used to determine the stability of the steady state solution for the chosen resonance case. The time delay is an efficient agent when choosing the absorber. They detected that there is a critical value in which the effectiveness of suppressing vibration is below based on using the influence of time delay on the main system's behavior. Amer and Soliman [15] discussed the impact of the time delay feedback control on the dynamical system's vibrations which consists of two degrees of freedom under the effect of parametric force. Employing the perturbation approach to get the second order approximations for the system's response. Stability among the pendulum and the main system is studied near the state of 1:2 sub-harmonic resonances. Their results shown that when the saturation control is invalid, time-delayed control could be employed to stabilize the system or reduce vibration. Moreover, the discussion of suppressing vibration at several values of delay is studied.

Lately, various controllers of time delay and active control are employed for controlling the vibrations of the nonlinear systems of cantilever beam inside moderated lumped mass by means of numerous researchers [16-18]. Liu et al. [16] added mixed of the time delay feedback control of displacement and velocity within a cantilever beam loading a lumped mass. They were able to obtain the analytical solutions for the beam in primary, superharmonic, and subharmonic resonance states by employing the multiple scales technique. Additionally, the top peak amplitude is moving to a short recurrence by the coefficient of displacement feedback and the vibrational stability and reduced the model's nonlinear vibrations are achieved by utilizing the coefficient of velocity feedback and their time delays. Hamed et al. [17] studied the applying of a nonlinear modified positive position feedback (MPPF) control onto a cantilever beam loading a lumped mass. According to their results the (MPPF) control is more efficient in suppressing performance, and



it is more effective in reducing the vibrations than the positive position feedback (PPF). Moreover, Hany and Ashraf [18] applied both Integral Resonant Control (IRC) and Nonlinear Saturation Control (NSC) on the model of the cantilever beam. The perturbation approach is utilized to get the (FRE) near the simultaneous resonance. The results from the novel controller (IRC+NSC) are superior to those of (NSC), (IRC), Negative velocity feedback (NVF), and Negative displacement feedback (NDF) in terms of suppressing the vibrations of the model's beam. By using the nonlinear saturation control (NSC), Saeed et al. [19] added a time delay to the process of controlling to repress nonlinear beam vibrations. The closed loop system's stability had been assessed by doing a bifurcation analysis. It is discussed how effective the time delay was. Also, Saeed et al. [20] examined a mix of the position and velocity time delay feedback into the cantilever beam. using the homotopy technique to get the equation for the controlled beam's motion. several resonance cases are discussed to get the amplitude and phase equations for the system's dynamics. They showed from their obtained analytical

findings that the loop delay has a significant impact on the controller's effectiveness.

That work was planned in the following manner: In Section 2, the mathematical paradigm of the beam system under the impact of external forcing after the addition of the negative velocity feedback control is discussed, thereafter using the multiple scale approach and its solution up to the second order approximation is studied. In section 3, the frequency response equation is obtained through the stability analysis of the beam at primary resonance case then the linear and nonlinear stability solutions are investigated. In Section 4, the numerical results and impacts of the system's parameters on the oscillating beam system are presented and discussed to show the optimization conditions for suppressing the system's vibration. In Section 5, the mathematical paradigm of the beam system after the addition of the time delay velocity controller with its solutions to obtain the (FRE) then discussing the efficient zone of time delay and the time delay's impact on the beam system are studied. Lastly, Section 6 displays the conclusions.

7798

## 2. Mathematical paradigm with negative velocity feedback control (NVF)

The beam paradigm exposed to pivotal force  $F(t)$  utilizing the piezoelectric substance is displayed in Fig. 1. The influence of the external forcing ( $F(t) = F_0 \cos(\Omega t)$ ) has applied over the pivotal direction at the location ( $x = x_F$ ) of the basis beam. The basis beam's substance is isotropic and homogeneously distributed. There is a nonlinear differential equation in Ref[7] that described the motion of the beam system's dynamic behavior. the dynamical beam motion's modified equation after the addition of the negative velocity feedback control  $R$  is displayed by:

$$\ddot{W} + 2\xi_1\omega_1 \dot{W} + \omega_1^2 W + \alpha W \dot{W} + \beta W^2 + \gamma W^3 = F \cos(\Omega t) + R \quad (1)$$

Where  $W$  is the displacement of the beamsystem,  $\xi_1$  is the damping coefficient,  $\omega_1$  is the natural frequency,  $\alpha, \beta, \gamma$  are parameters of the nonlinearity,  $F$  is the external forcing amplitude,  $\Omega$  is the excitation frequency of the beam system,

( $R = -GW^n; n = 1, 3$ ) is the input of the control,  $G$  is a coefficient of the gain, and  $\varepsilon$  is a perturbation parameter.

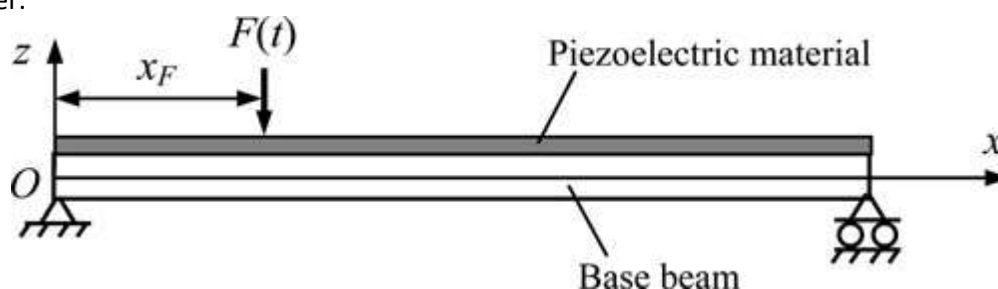


Fig.1 graphic model for the nonlinear beam attached with the piezoelectric substance under the effect of pivotal force

**2.1. Perturbation procedure**

Because of the appearance of the beam system parameters in the following perturbation equations when utilizing (MSP), the parameters are scaled as follows:

$$\xi_1 = \varepsilon \hat{\xi}_1, \alpha = \varepsilon \hat{\alpha}, \beta = \varepsilon \hat{\beta}, \gamma = \varepsilon \hat{\gamma}, F = \varepsilon \hat{F}, G = \varepsilon \hat{G}$$

The (MSP) approach [20, 21] is used to get the solution of equation (1) to the second-order expansion, the expansion of W(t) as into the next shape:

$$W(t; \varepsilon) = W_0(T_0, T_1, T_2) + \varepsilon W_1(T_0, T_1, T_2) + \varepsilon^2 W_2(T_0, T_1, T_2) + O(\varepsilon^3) \tag{2}$$

where  $T_0 = t, (T_1 = \varepsilon t, T_2 = \varepsilon t^2)$  are the fast and slow time scales respectively. Time derivatives are given by:

$$\frac{d}{dt} = D_0 + \varepsilon D_1 + \varepsilon^2 D_2, \frac{d^2}{dt^2} = D_0^2 + 2\varepsilon D_0 D_1 + \varepsilon^2 (D_1^2 + 2D_0 D_2) \tag{3}$$

where  $D_s = \frac{\partial}{\partial T_s}, s = (0, 1, 2)$

Substituting equations (2),(3) in equation (1) subsequently, equalizing the  $\varepsilon$  parameters drive to:

$$\varepsilon^0 : (D_0^2 + \omega_1^2) W_0 = 0 \tag{4a}$$

$$\varepsilon^1 : (D_0^2 + \omega_1^2) W_1 = -2D_0 D_1 W_0 - 2\hat{\xi}_1 \omega_1 D_0 W_0 - \hat{\alpha} W_0 D_0 W_0 - \hat{\beta} W_0^2 - \hat{\gamma} W_0^3 + \hat{F} \cos(\Omega t) - \hat{G} (D_0 W_0)^3 \tag{4b}$$

$$\varepsilon^2 : (D_0^2 + \omega_1^2) W_2 = -2D_0 D_1 W_1 - D_1^2 W_0 - 2D_0 D_2 W_0 - 2\hat{\xi}_1 \omega_1 (D_0 W_1 + D_1 W_0) - \hat{\gamma} (3 W_0^2 W_1) - \hat{\alpha} (W_0 (D_0 W_1 + D_1 W_0) + W_1 (D_0 W_0)) - \hat{G} [3(D_0 W_0)^2 (D_0 W_1 + D_1 W_0)] \tag{4c}$$

The (equation (4a))'s solution is presented through:  $W_0 = A(T_1, T_2) e^{i\omega_1 T_0} + \bar{A}(T_1, T_2) e^{-i\omega_1 T_0}$

where  $A$  is unknown function into both of  $T_1, T_2$ .

Substituting equation (5) in (4b) yields:

$$(D_0^2 + \omega_1^2) W_1 = (-2i \omega_1 D_1 A - 2i \hat{\xi}_1 \omega_1^2 A - 3\hat{\gamma} A^2 \bar{A} - 3i \hat{G} \omega_1^3 A^2 \bar{A}) e^{i\omega_1 T_0} + \left(\frac{\hat{F}}{2}\right) e^{i\Omega T_0} - (i \hat{\alpha} \omega_1 A^2 + \hat{\beta} A^2) e^{2i\omega_1 T_0} - (\hat{\gamma} A^3 + i \hat{G} \omega_1^3 A^3) e^{3i\omega_1 T_0} - 2\hat{\beta} A \bar{A} + cc \tag{6}$$

where  $cc$  refers to the complex conjugate parameters for the previous terms. To get a bounded solution, we should delete the secular terms and the public solution for equation (6) is formulated in the following:

$$W_1 = M_1(T_1, T_2) e^{2i\omega_1 T_0} + M_2(T_1, T_2) e^{3i\omega_1 T_0} + M_3(T_1, T_2) e^{i\Omega T_0} + M_4(T_1, T_2) + cc \tag{7}$$

where  $M_s (s = 1, 2, \dots, 4)$  are complex functions into both of  $T_1, T_2$  that are defined into Appendix.

Substituting equations (5) and (6) in (4c) we get:

$$(D_0^2 + \omega_1^2) W_2 = \left[ -2i \omega_1 D_2 A - 2\hat{\xi}_1 \omega_1 D_1 A - D_1^2 A - i \hat{\alpha} \omega_1 E_1 \bar{A} - i \hat{\alpha} \omega_1 A (E_4 + \bar{E}_4) - 2\hat{\beta} A (E_4 + \bar{E}_4) - 3\hat{\gamma} \bar{A}^2 E_2 + 3\hat{G} \omega_1^2 A^2 (D_1 \bar{A}) - 6\hat{G} \omega_1^2 A \bar{A} (D_1 A) \right] e^{i\omega_1 T_0} + \left[ -4i \omega_1 (D_1 E_1) - 4i \hat{\xi}_1 \omega_1^2 E_1 - \hat{\alpha} A (D_1 A) - 2i \hat{\alpha} \omega_1 E_2 \bar{A} - 2\hat{\beta} \bar{A} E_2 - 3\hat{\gamma} A^2 (E_4 + \bar{E}_4) \right] e^{i\omega_1 T_0}$$



$$\begin{aligned}
 & -6\hat{\gamma}A\bar{A}E_1 - 2i\hat{G}\omega_1^3E_1A\bar{A}]e^{2i\omega_1T_0} + [-6i\omega_1(D_1E_2) - 6i\hat{\xi}_1\omega_1^2E_2 - 2\hat{\beta}AE_1 \\
 & - 3i\hat{\alpha}\omega_1E_1A - 6\hat{\gamma}A\bar{A}E_2 + 3\hat{G}\omega_1^2A^2(D_1A) - 18i\hat{G}\omega_1^3E_2A\bar{A}]e^{3i\omega_1T_0} \\
 & + [-3\hat{\gamma}A^2E_1 - 2\hat{\beta}AE_2 - 4i\hat{\alpha}\omega_1AE_2 + 6i\hat{G}\omega_1^3A^2E_1]e^{4i\omega_1T_0} + [-3\hat{\gamma}A^2E_2 \\
 & + 9i\hat{G}\omega_1^3A^2E_2]e^{5i\omega_1T_0} + [-2i\Omega(D_1E_3) - 2i\hat{\xi}_1\omega_1\Omega E_3 - 6\hat{\gamma}A\bar{A}E_3 \\
 & - 6i\hat{G}\omega_1^2\Omega E_3A\bar{A}]e^{i\Omega T_0} + [-i\Omega\hat{\alpha}AE_3 - i\hat{\alpha}\omega_1AE_3 - 2\hat{\beta}E_3A]e^{i(\Omega+\omega_1)T_0} \\
 & + [-i\Omega\hat{\alpha}\bar{A}E_3 + i\hat{\alpha}\omega_1\bar{A}E_3 - 2\hat{\beta}E_3\bar{A}]e^{i(\Omega-\omega_1)T_0} + [3i\hat{G}\Omega E_3\omega_1^2A^2 \\
 & - 3\hat{\gamma}A^2E_3]e^{i(\Omega+2\omega_1)T_0} + [3i\hat{G}\Omega E_3\omega_1^2\bar{A}^2 - 3\hat{\gamma}\bar{A}^2E_3]e^{i(\Omega-2\omega_1)T_0} + 6i\hat{G}\omega_1^3E_1\bar{A}^2 \\
 & - \hat{\alpha}\bar{A}(D_1\bar{A} + D_1A) - 6\hat{\gamma}A\bar{A}(E_4 + \bar{E}_4) - 3\hat{\gamma}\bar{A}^2E_1 + cc \quad (8)
 \end{aligned}$$

After removing the secular terms from equation (8), the public solution for this equation is acquired in the following:

$$\begin{aligned}
 W_2 = & K_1e^{2i\omega_1T_0} + K_2e^{3i\omega_1T_0} + K_3e^{4i\omega_1T_0} + K_4e^{5i\omega_1T_0} + K_5e^{i\Omega T_0} + K_6e^{i(\Omega+\omega_1)T_0} + K_7e^{i(\Omega-\omega_1)T_0} \\
 & + K_8e^{i(\Omega+2\omega_1)T_0} + K_9e^{i(\Omega-2\omega_1)T_0} + K_{10} + cc \quad (9)
 \end{aligned}$$

where  $K_j$  ( $j=1,2,\dots,10$ ) are complex functions into both of  $T_1, T_2$  that are presented into Appendix.

The majority of the resonance cases that taken from the approximate solutions got up above are categorized into the following:

- (a) Primary resonance:  $\Omega \cong \omega_1$
- (b) Sub-harmonic resonance:  $\Omega \cong 2\omega_1, \Omega \cong 3\omega_1$

### 3. Stability analysis

The steady-state solution's stability in the case of primary resonance ( $\Omega \cong \omega_1$ ) are discussed. As a result, we input the detuning parameter  $\sigma_1$  in this relationship:

$$\Omega = \omega_1 + \sigma_1 = \omega_1 + \varepsilon\hat{\sigma}_1 \quad (10)$$

where  $\sigma_1$  represents the nearness of  $\Omega$  to  $\omega_1$ . obtaining the solvability conditions by putting equation (10) in equation (6) then scaling each parameter back to its authentic value, we acquire

$$-2i\omega_1D_1A - 2i\xi_1\omega_1^2A - 3\gamma A^2\bar{A} - 3iG\omega_1^3A^2\bar{A} + \frac{F}{2}e^{i\sigma_1T_1} = 0 \quad (11)$$

Expressing A into this polar form as :

$$A = \left(\frac{a}{2}\right) e^{i\varphi} \quad (12)$$

where  $a, \varphi$  are the amplitude and phase for the beam system, respectively.

Substituting equation (12) in equation (11), thereafter isolating real and imaginary parts yields:

$$\dot{a} = -\xi_1\omega_1a - \frac{3G\omega_1^2a^3}{8} + \frac{F}{2\omega_1}\sin(\theta_1) \quad (13a)$$

$$a\dot{\varphi} = \frac{3\gamma a^3}{8\omega_1} - \frac{F}{2\omega_1}\cos(\theta_1) \quad (13b) \text{ where}$$

$$\theta_1 = \hat{\sigma}_1T_1 - \varphi = \sigma_1t - \varphi \Rightarrow \dot{\varphi} = \sigma_1 - \dot{\theta}_1 \quad (14)$$

Substituting equation (14) in equations (13), we get:



$$\dot{a} = -\xi_1 \omega_1 a - \frac{3G \omega_1^2 a^3}{8} + \frac{F}{2\omega_1} \sin(\theta_1) \quad (15a)$$

$$a \dot{\theta}_1 = a \sigma_1 - \frac{3\gamma a^3}{8\omega_1} + \frac{F}{2\omega_1} \cos(\theta_1) \quad (15b)$$

By setting ( $\dot{a} = \dot{\theta}_1 = 0$ ) in equations (15) to arrive to the beam system steady-state solution.

$$\left(\xi_1 \omega_1 a + \frac{3G \omega_1^2 a^3}{8}\right) = \frac{F}{2\omega_1} \sin(\theta_1) \quad (16a)$$

$$\left(a \sigma_1 - \frac{3\gamma a^3}{8\omega_1}\right) = -\frac{F}{2\omega_1} \cos(\theta_1) \quad (16b) \text{ By solving those}$$

equations (16), we acquire the frequency-response equation (FRE):

$$\left(\xi_1 \omega_1 a + \frac{3G \omega_1^2 a^3}{8}\right)^2 + \left(a \sigma_1 - \frac{3\gamma a^3}{8\omega_1}\right)^2 - \frac{F^2}{4\omega_1^2} = 0 \quad (17)$$

### 3.1. Linear solution stability

For explaining the acquired fixed points for the linear solution's stability, suppose that one:

$$A(T_1, T_2) = \left(\frac{p_1 - ip_2}{2}\right) e^{i\Psi T_1} \quad (18)$$

where  $p_1$  and  $p_2$  are genuine values then taking into our consideration that  $\Psi = \sigma_1$ .

Substituting equation (18) in the (equation (11)) 's linear part and isolating both of real and imaginary pieces, we acquire :

$$\dot{p}_1 = -(\hat{\xi}_1 \omega_1) p_1 + (-\hat{\sigma}_1) p_2 \quad (19a)$$

$$\dot{p}_2 = (\hat{\sigma}_1) p_1 - (\hat{\xi}_1 \omega_1) p_2 + \frac{\hat{F}}{2\omega_1} \quad (19b)$$

The zero distinctive equations are used to get the linear solution's stability:

$$\begin{vmatrix} -\hat{\xi}_1 \omega_1 - \lambda & -\hat{\sigma}_1 \\ \hat{\sigma}_1 & -\hat{\xi}_1 \omega_1 - \lambda \end{vmatrix} + \frac{\hat{F}}{2\omega_1} = 0 \quad (20)$$

$$\text{where } \lambda_{1,2} = -(\hat{\xi}_1 \omega_1) \pm i \left(\hat{\sigma}_1 + \sqrt{\frac{\hat{F}}{2\omega_1}}\right)$$

because the value of  $(\hat{\xi}_1 \omega_1)$  is positive, the solutions are stable.

### 3.3. Nonlinear solution stability

For determining stability for the nonlinear solutions' fixed points, we make the next assumption:

$$a = a_{10} + a_{11}, \theta_1 = \theta_{10} + \theta_{11} \quad (21)$$

7801

where  $a_{10}, \theta_{10}$  are the solutions for equations (16). Inserting equations (21) in equations (15) with preserving the linear terms that exist only into  $a_{11}, \theta_{11}$ , we obtain:

$$\dot{a}_{11} = \left(-\xi_1 \omega_1 - \frac{9G \omega_1^2 a_{10}^2}{8}\right) a_{11} - \left(\frac{F}{2\omega_1} \cos(\theta_{10})\right) \theta_{11} \quad (22a)$$

$$\dot{\theta}_{11} = \left(\frac{\sigma_1}{a_{10}} - \frac{9\gamma}{8\omega_1} a_{10}\right) a_{11} - \left(\frac{F}{2\omega_1 a_{10}} \sin(\theta_{10})\right) \theta_{11} \quad (22b)$$



The zero distinctive equations are utilized to obtain the nonlinear solution's stability:

$$\begin{vmatrix} -\xi_1 \omega_1 - \frac{9G \omega_1^2 a_{10}}{8} - \lambda & -\frac{F}{2\omega_1} \cos(\theta_{10}) \\ \frac{\sigma_1}{a_{10}} - \frac{9\gamma a_0}{8\omega_1} & -\frac{F}{2\omega_1 a_{10}} \sin(\theta_{10}) - \lambda \end{vmatrix} = 0 \quad (23)$$

Obtaining the eigenvalues to equations (23) from this relation:

$$\lambda^2 + r_1 \lambda + r_2 = 0 \quad (24)$$

where  $r_1, r_2$  are the coefficients of equation(24) that obtain from Appendix.

As a result, the nonlinear solution's stability is obtained if the real part of the eigenvalues is negative. Else, it is unstable.

#### 4

#### . Results and discussions

During that department, a discussion of the numerical solutions for the beam system behavior of equation (1) is studied by applying Runge-Kutta fourth -order approach that utilizes Maple16 software and M ATLAB7.7(R2014) prior and after the control at the determined values:

$$\xi_1 = 0.03, \alpha = 0.01, \beta = 0.5, \gamma = 0.6, \omega_1 = 3, \Omega = \omega_1, F = 9, G = 5, k_1 = 5$$

#### 4.1. Absence of beam system control

Fig. 2 displays the beam system response and its phase-plane in the absence of the beam system control near the case  $\Omega \cong \omega_1$ . Through that figure, we sight that the amplitude for the beam system with no control is about 30% from the external force F, and the phase plane shows stability accompanied by several limit cycles.

7802

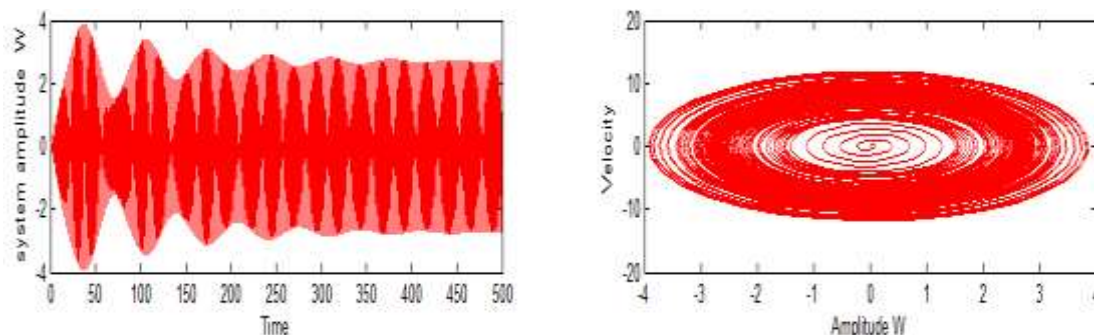


Fig. 2 Beam system behavior before control at the case  $\Omega \cong \omega_1$

#### 4.2. Impact of beam system control

Fig.3 demonstrates the beam system response and its phase-plane in the existence of cubic velocity feedback control near the resonance case  $\Omega \cong \omega_1$ . From that figure, it can be seen that the amplitude for the beam system is nearly 5% from the external force F. Also, we sight that the steady-state amplitude was reduced from 2.684 which shown in Fig. 2 to nearly 0.4434 as shown in Fig. 3. As a result, comparing Fig. 2 with Fig. 3 make a best suppression of vibration of amplitude. So, the

efficiency for the control is  $E_a$  ( $E_a$  = steady-state amplitude for the beam system with no control/ steady-state amplitude for the beam system with control) is nearly 6. Fig. 4 displays the effective of linear and cubic velocity feedback control. Through that figure it can be sight that the control of cubic velocity ( $R = -G\dot{W}^n; n = 3$ ) is the best when compared with the control of linear velocity ( $R = -G\dot{W}^n; n = 1$ ).



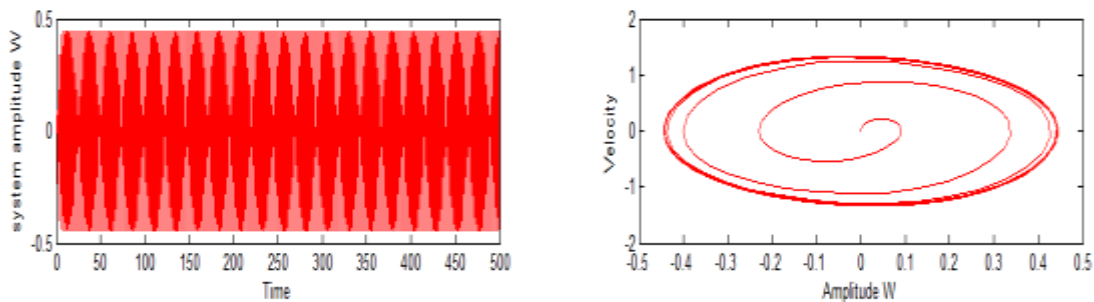


Fig. 3 Beam system behavior after control at resonance case  $\Omega \cong \omega_1$

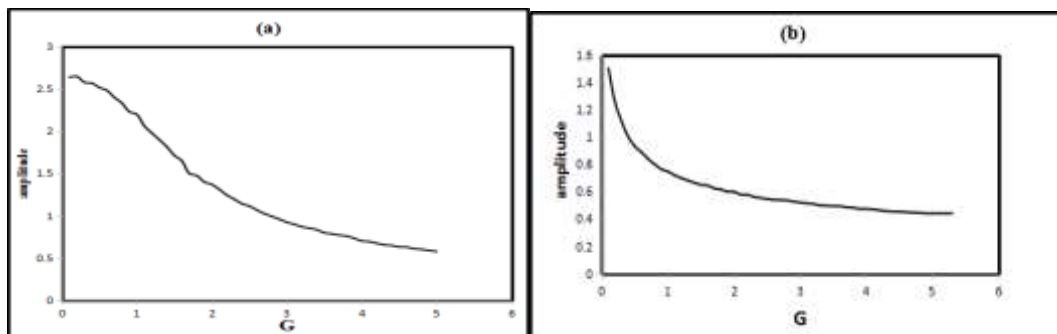


Fig. 4 Comparison between linear and cubic feedback control  
 (a) linear feedback control ( $R = -GW^n; n = 1$ ) (b) cubic control ( $R = -GW^n; n = 3$ )

### 4.3. Frequency response curves

In that part, we will present all of the curves of the response curves that occurred in the studied beam system prior and after the addition of the controller. The (FRE) that is given in equation (17) are solved by utilizing Maple (16) software for the steady-state amplitude  $a$  against the detuning parameter  $\sigma_1$  as illustrated in Figs. 5, 7. Fig. 5 displays the beam system's response curves in the absence of the control into equation (17) at the external forcing amplitude  $F$  impact's different values. It is observed that increasing values for the external forcing amplitude  $F$  increase the beam system's steady-state amplitude. In addition, the response curve bends over to the right that lead to a hard spring, and the jump phenomena is plainly visible because of the nonlinearity's dominance. Fig. 6 shows a comparison of the FRC in the absence of the control and under the impact of control for the beam system. We have good amplitude vibration suppression under the effect of control as seen in that figure. The impacts of several beam's parameters under the impact of control are discussed in Fig. 7. Fig. 7a displayed the growing of the amplitude (a) when the values

of external forcing amplitude  $F$  increase. As illustrated in Figs. 7b, 7d, the curves narrow with reducing of the peak amplitude (a) when rising values of the damping coefficient  $\xi_1$  and gain coefficient  $G$  for the beam system. As a result, the amplitude (a) are inversely proportion to these coefficients, which are accord well with the results in Fig. 4. Also, as shown in Fig. 7c reducing the values of natural frequency  $\omega_1$  leads to a decrease in the amplitude (a) of the beam system, and the curve becomes more extensive as the peak of the natural frequency decreases. Furthermore, we explored no alteration in the FRC of the beam system under the effect of control if the values of nonlinear parameters  $\alpha, \beta$  and  $\gamma$  changed. Finally, the response curves of the external forcing amplitude  $F$  against the amplitude (a) for the beam system prior and after the impact of control is shown in Fig. 8 by utilizing the condition  $\sigma_1 = 0$ . We noticeable before utilizing the impact of the controller, the relationship between the beam system amplitude (a) and the external forcing amplitude  $F$  was determined to be nonlinear. This results in a large amplitude (a)



for the beam system due to a slight raise in values of external forcing amplitude  $F$ . But after employing the control makes the

amplitude( $a$ )for the beam system decreases,so the cubic velocity feedback control is a strong mechanism for minimizing the vibration.

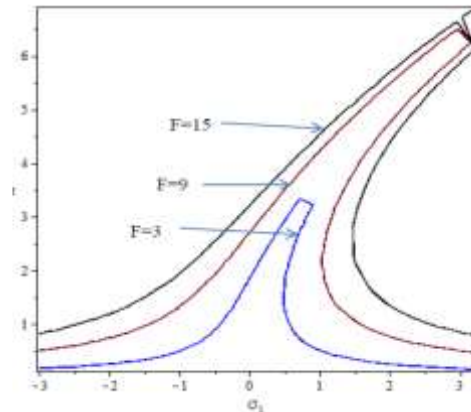


Fig.5 Impact of external forcing amplitude  $F$  in the absence of the control

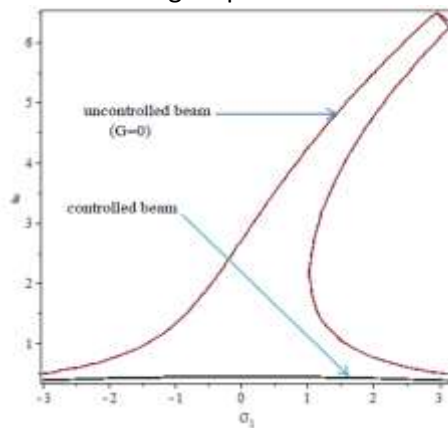
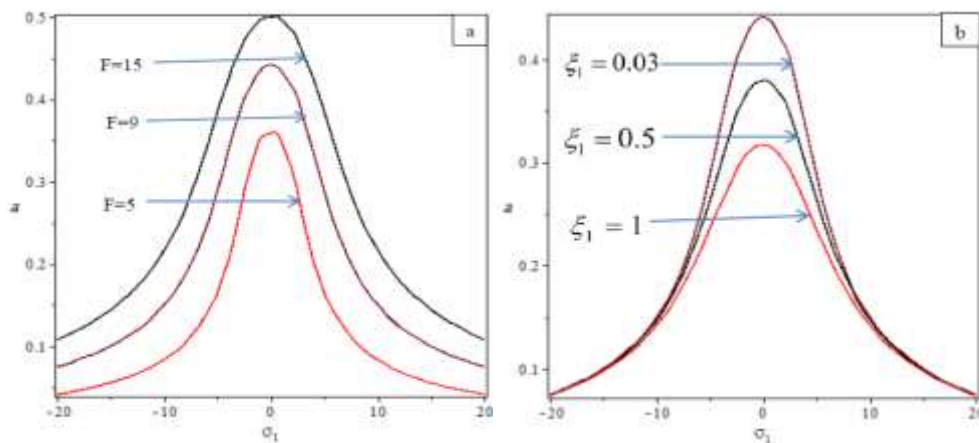


Fig.6 Comparison of the FRC in the absence of control and with using control of the beam system



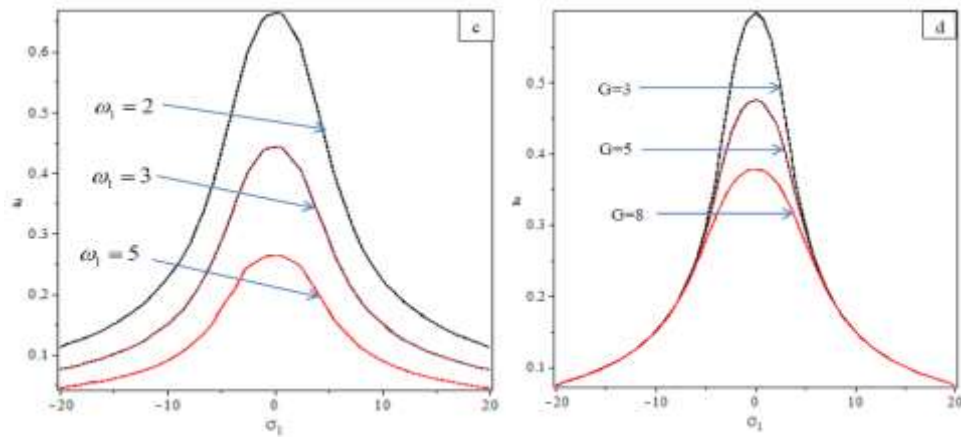


Fig.7 Impacts of several parameters of the FRC after utilizing the control of the beam system (a against  $\sigma_1$ )

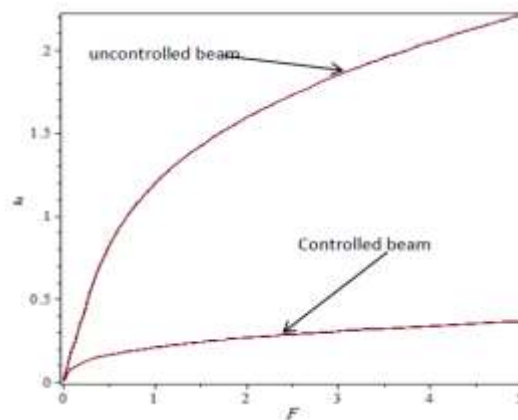


Fig. 8 Excitation forcing amplitude response curves in the absence of control and after utilizing the control of the beam system at  $\sigma_1 = 0$

**4.4. Comparing analytical solution and the numerical simulation**

Fig. 9 demonstrates comparing the analytical solution which is presented through equation (15) by utilizing (MSPT) at the resonance case  $\Omega \cong \omega_1$  and the numerical simulation of

equation (1) through employing Runge-Kutta technique. The dashed line represents the analytical solution while the numerical simulation represents by the solid line. We can sight from this figure that the analytical and numerical solution agrees fairly well.

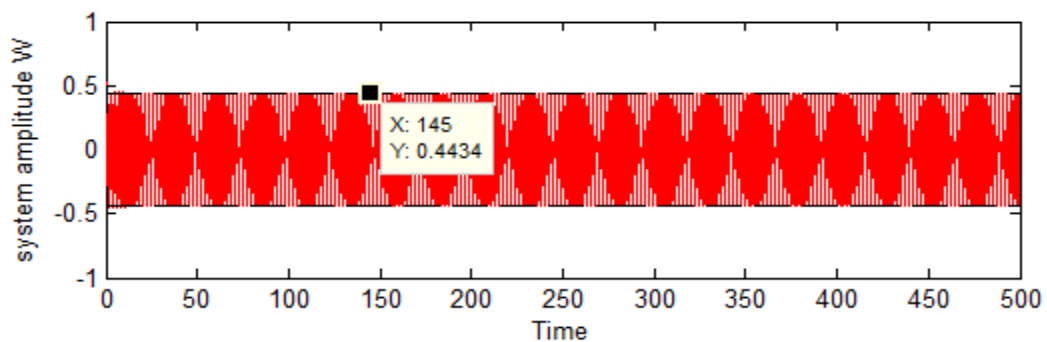


Fig. 9 comparing the analytical and numerical solution under the impact of control at  $\Omega \cong \omega_1$  (----- analytical solution, \_\_\_\_\_ numerical simulation)



### 5. Mathematical paradigm with time delay velocity feedback

$$\ddot{W} + 2\xi_1 \omega_1 \dot{W} + \omega_1^2 W + \alpha W \dot{W} + \beta W^2 + \gamma W^3 = F \cos(\Omega t) + k_1 \dot{W}(t - \tau) \quad (25)$$

Where  $k_1 = \varepsilon \hat{k}_1$  is the control gain coefficient,  $\tau$  is the time delay for the control

$$\xi_1 = \varepsilon \hat{\xi}_1, \alpha = \varepsilon \hat{\alpha}, \beta = \varepsilon \hat{\beta}, \gamma = \varepsilon \hat{\gamma}, F = \varepsilon \hat{F}.$$

Employing the (MSPT), we acquire a second-order uniform expansion for the solutions of equation (25) by this formula:

$$W(t; \varepsilon) = W_0(T_0, T_1, T_2) + \varepsilon W_1(T_0, T_1, T_2) + \varepsilon^2 W_2(T_0, T_1, T_2) \quad (26)$$

$$W(t - \tau; \varepsilon) = W_{0\tau}(T_0 - \tau, T_1 - \varepsilon\tau, T_2 - \varepsilon^2\tau) + \varepsilon W_{1\tau}(T_0 - \tau, T_1 - \varepsilon\tau, T_2 - \varepsilon^2\tau) + \varepsilon^2 W_{2\tau}(T_0 - \tau, T_1 - \varepsilon\tau, T_2 - \varepsilon^2\tau) \quad (27)$$

where  $T_n = \varepsilon^n t$ , ( $n = 0, 1, 2$ ) are the time scales while the time derivatives are given through:

$$\frac{d}{dt} = D_0 + \varepsilon D_1 + \varepsilon^2 D_2, \frac{d^2}{dt^2} = D_0^2 + 2\varepsilon D_0 D_1 + \varepsilon^2 (D_1^2 + 2D_0 D_2) \quad (28)$$

Substituting equations (26)-(28) in equation (25), thereafter, equalizing the  $\varepsilon$  parameters drive to:

$$\varepsilon^0 : (D_0^2 + \omega_1^2) W_0 = 0 \quad (29a)$$

$$\varepsilon^1 : (D_0^2 + \omega_1^2) W_1 = -2D_0 D_1 W_0 - 2\hat{\xi}_1 \omega_1 D_0 W_0 - \hat{\alpha} W_0 D_0 W_0 - \hat{\beta} W_0^2 - \hat{\gamma} W_0^3 + \hat{F} \cos(\Omega t) + \hat{k}_1 (D_0 W_{0\tau}) \quad (29b)$$

$$\varepsilon^2 : (D_0^2 + \omega_1^2) W_2 = -2D_0 D_1 W_1 - D_1^2 W_0 - 2D_0 D_2 W_0 - 2\hat{\xi}_1 \omega_1 (D_0 W_1 + D_1 W_0) + W_1 (D_0 W_0) - \hat{\alpha} (W_0 (D_0 W_1 + D_1 W_0)) - \hat{\beta} (2 W_0 W_1) - \hat{\gamma} (3 W_0^2 W_1) + \hat{k}_1 (D_0 W_{1\tau} + D_1 W_{0\tau}) \quad (29c)$$

The (equation (29a))'s solution is presented through:

$$W_0 = A(T_1, T_2) e^{i\omega_1 T_0} + \bar{A}(T_1, T_2) e^{-i\omega_1 T_0} \quad (30)$$

7806

From equation (30) the time delay feedback's solution is displayed as:

$$W_{0\tau} = A(T_1 - \varepsilon\tau, T_2 - \varepsilon^2\tau) e^{i\omega_1 (T_0 - \tau)} + \bar{A}(T_1 - \varepsilon\tau, T_2 - \varepsilon^2\tau) e^{-i\omega_1 (T_0 - \tau)} \quad (31)$$

where  $A, \bar{A}(T_1 - \varepsilon\tau, T_2 - \varepsilon^2\tau)$  are unbeknown functions into both of  $T_1, T_2$ .

Substituting equations (30) and (31) in equation (29b) yields:

$$(D_0^2 + \omega_1^2) W_1 = (-2i \omega_1 D_1 A - 2i \hat{\xi}_1 \omega_1^2 A - 3\hat{\gamma} A^2 \bar{A} + i \omega_1 \hat{k}_1 A e^{-i\omega_1 \tau}) e^{i\omega_1 T_0} + \left(\frac{\hat{F}}{2}\right) e^{i\Omega T_0} - (i \hat{\alpha} \omega_1 A^2 + \hat{\beta} A^2) e^{2i\omega_1 T_0} - (\hat{\gamma} A^3) e^{3i\omega_1 T_0} - 2\hat{\beta} A \bar{A} + cc \quad (32)$$

To get rid of the secular term, then scaling each parameter back to its authentic value, we acquire:

$$D_1 A = -\xi_1 \omega_1 A + \frac{k_1 A}{2} e^{-i\omega_1 \tau} - i \frac{3\gamma A^2 \bar{A}}{2\omega_1} - i \frac{F}{4\omega_1} e^{i\sigma T_1} \quad (33)$$

Substituting from  $A = \left(\frac{a}{2}\right) e^{i\varphi}$  in equation (33), thereafter isolating real and imaginary part, we arrive at:

$$\dot{a} = -\xi_1 \omega_1 a + \left(\frac{k_1 a}{2}\right) \cos(\omega_1 \tau) + \left(\frac{F}{2\omega_1}\right) \sin(\theta_1) \quad (34a)$$

$$a \dot{\theta}_1 = a \sigma_1 - \frac{3\gamma a^3}{8\omega_1} + \left(\frac{k_1 a}{2}\right) \sin(\omega_1 \tau) + \left(\frac{F}{2\omega_1}\right) \cos(\theta_1) \quad (34b)$$

where  $\theta_1 = \sigma T_1 - \varphi$

The beam system steady-state solution is reached by setting  $\dot{a} = \dot{\theta}_1 = 0$  in equation (34):



$$\xi_1 \omega_1 a = \frac{k_1 a}{2} \cos(\omega_1 \tau) + \frac{F}{2\omega_1} \sin(\theta_1) \tag{35a}$$

$$(a\sigma_1 - \frac{3\gamma a^3}{8\omega_1}) = -\frac{k_1 a}{2} \sin(\omega_1 \tau) - \frac{F}{2\omega_1} \cos(\theta_1) \tag{35b}$$

Then we have

$$\frac{9\gamma^2 a^6}{64\omega_1^2} - \frac{6\gamma\sigma_1 a^4}{8\omega_1} + (\sigma_1^2 + \xi_1^2 \omega_1^2 - \frac{k_1^2}{4}) a^2 - (\frac{Fk_1 a}{2\omega_1} \sin(\omega_1 \tau + \theta_1)) a - \frac{F^2}{4\omega_1^2} = 0 \tag{36}$$

**5.1. Numerical results**

Fig. 8 depicts how the velocity feedback control's time delay affects the beam system's amplitude, and it is clear that the time delay's most effective regions are  $0.6 \leq \tau \leq 1.4, 2.8 \leq \tau \leq 3.3$ . Outside of this range, the beam system's steady state amplitude grows with a few chaos and

occasionally results in instability. Therefore, we take  $\tau = 1.1$  as illustrated in Fig.9, the amplitude is reduced and the minimum value is close to 0.573 and hence  $E_a = 4.7$ , which indicates that the control of negative cubic velocity feedback is superior to the time delay control.

7807

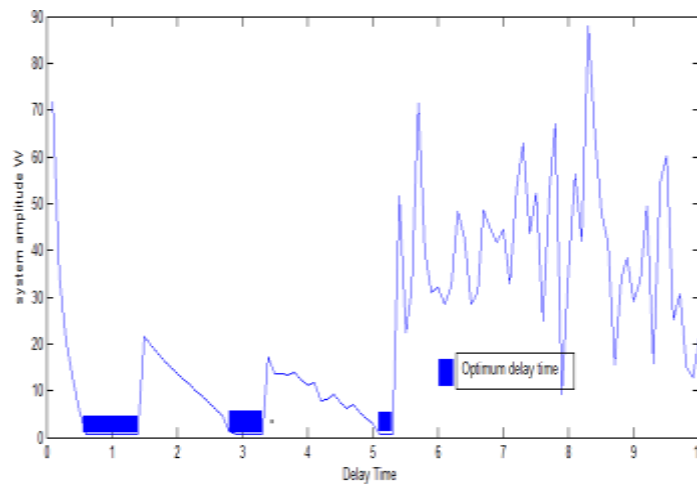


Fig.8 Impact of time delay

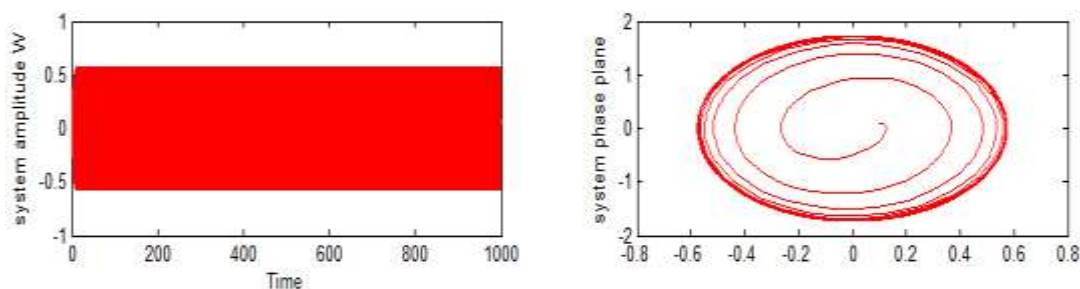


Fig. 9 Primary resonance case  $\Omega \cong \omega_1$  with time delay control ( $\tau = 1.1$ )

**6. Conclusions**

Both the velocity feedback controller and time delay control were employed in that work in order to lessen the vibrations for a nonlinear beam. The multiple scales approach is utilized to acquire the second-order approximate solutions for the specified beam system. Stability investigation is discussed close to the

primary resonance case to obtain the FRE. Also, the beam system's stability behavior utilizing the FRC was illustrated. It was numerically investigated how various parameters affected the frequency response curves prior to and after the control. The following findings from the aforementioned study might be concluded:



1. The existence of the velocity feedback control for the beam system has reduced the amplitude from 2.684 which is shown in Fig. 2 to nearly 0.4434 as displayed in Fig. 3. As a result, comparing Fig. 2 with Fig. 3 makes the best suppression for the vibration amplitude.
2. The efficient region for time delay are  $0.6 \leq \tau \leq 1.4, 2.8 \leq \tau \leq 3.3$ , and the time delay controller's efficiency is  $E_a = 4.7$ , whereas the cubic velocity feedback controller's efficiency is  $E_a = 6$ . Therefore, a control using cubic velocity feedback is superior to the time delay control.
3. The control of cubic velocity feedback is superior to the linear velocity feedback.
4. Increasing values for the external forcing amplitude  $F$  increase the beam system's steady-state amplitude ( $a$ ) in the absence of control. In addition, the response curve bends over to the right which leads to a hard spring, and the jump phenomena is plainly visible because of the nonlinearity's dominance.
5. The beam system's amplitude ( $a$ ) under the impact of control is inversely proportion to these coefficients  $\xi_1, G, \omega_1$ , but it is directly proportion to the external forcing amplitude  $F$ .
6. Before utilizing the impact of the controller, the relationship between the beam system amplitude ( $a$ ) and the external forcing amplitude  $F$  was determined to be nonlinear. This results in a large amplitude ( $a$ ) for the beam system due to a slight raise in values of external forcing amplitude  $F$ . but after employing the control makes the amplitude ( $a$ ) for the beam system decreases.
7. When compared, the analytical and numerical solution is fairly in agreement, as seen in Fig.9.

## References

- [1] E. Ott, C. Grebogi and J. A. Yorke, Controlling chaos, Physical Review Letters 64 (1990) 1196- 1199.
- [2] K. Pyragas, Continuous control of chaos by self-controlling feedback, Physics Letters A 170 (1992) 421- 428.
- [3] C.C. Fuh, P.C. Tung, Control chaos using differential geometrical method, Physical Review Letters 75 (1995) 2952-295.

[4] C.R. Fuller, S.J. Elliott and P.A. Nelson, Active Control of Vibration, Academic press, New York, 1997.

[5] S. Boccaletti, C. Grebogi, Y.C. Lai, H. Mancini and D. Maza, The control of chaos, Theory and applications, Physics Reports 329 (2000) 103-197.

[6] M.Eissa and M. Sayed, Vibration reduction of a three DOF nonlinear spring Pendulum, Communications in Nonlinear Science and Numerical Simulation 13(2) (2008) 465–488.

[7] Li. F. Ming, Y. Guo and Z. Yimin, Active control of nonlinear forced vibration in a flexible beam using piezoelectric material, Mechanics of Advanced Materials and Structures 23(3) (2016) 311-317.

[8] M. Yaman and S. Sen, Vibration control of a cantilever beam of varying orientation, Inter J Solids Struct 44 (2007) 1210-1220.

[9] U. H. Hegazy, Single-mode response and control of a hinged-hinged flexible beam, Arch Appl Mech 79 (2007) 335-345.

[10] U. H. Hegazy, Control of periodic and chaotic motions in a cantilever beam with varying orientation under principal parametric resonance, International Journal of Control Science and Engineering 6(2) (2016) 23-37.

[11] A. Maccari, Vibration control for parametrically excited Lienard systems, Int. J. of Non-linear Mechanics 41 (2006) 146-155.

[12] A. Maccari, Vibration amplitude control for a van der Pol-Duffing oscillator with time delay, Journal of Sound and Vibration 317(2008)20-29.

[13] W. El-Ganaini and H. A. El-Gohary, Vibration suppression via time delay absorber non-linear differential equations, Adv. Theo. Appl. Mech 4(2) (2011) 49-67.

[14] W. El- Ganaini and H. A. El-Gohary, Vibration suppression of dynamical system to multi- parametric excitations via time-delay absorber, Appl. Math. Model 36 (2012) 35-45.

[15] Y. A. Amer and S. M. Soleman, The time delayed feedback control to suppress the vibration of the autoparametric dynamical system, Scientific Research and Essays 10(15) (2015)489-500.

[16] C. X. Liu, Y. Yan and W. Q. Wang, primary and secondary resonance analyses of a cantilever beam carrying an intermediate



lumped mass with time delay feedback 97(2019)1175-1195.

[17] Y. S. Hamed, A. El Shery and M. Sayed, Nonlinear modified positive position feedback control of cantilever beam system carrying an intermediate lumped mass, Alexandria Engineering Journal 59(5)(2020)3847-3862.

[18] H. S. Bauomy and A. T. EL-Sayed, Mixed controller (IRC+NSC) involved in the harmonic vibration response cantilever beam model, Measurement and Control 53(9-10)(2020)1954-1967.

[19] N. A. Saeed , W. A. El-Ganini and M. Eissa, Nonlinear time delay saturation-based

controller for suppression of non-linear beam vibrations, Applied Mathematical Modelling 37(20-21)(2013)8846-8864.

[20]N. A. Saeed, G. M. Moatimid, F. M. F. Elsabaa and Y.Y. Ellabban, Time-delayed control to suppress a nonlinear system vibration utilizing the multiple scales homotopy approach, Archive of Applied Mechanics 91(2021)1193-1215.

[21] A. H. Nayfeh and D. T. Mook, Nonlinear oscillations, Wiley, New York, 1995.

[22] A. H. Nayfeh , Problems in Perturbation , Wiley, New York, 1985.

### Appendix

$$E_1 = \frac{i \hat{\alpha} \omega_1 A^2 + \hat{\beta} A^2}{3\omega_1^2}, E_2 = \frac{\hat{\gamma} A^3 - iG \omega_1^3 A^3}{8\omega_1^2}, E_3 = \frac{\hat{F}}{2(\omega_1^2 - \Omega^2)}, E_4 = \frac{-2\beta A \bar{A}}{\omega_1^2}$$

$$K_1 = \frac{-4i \omega_1 (D_1 E_1) - 4i \hat{\xi}_1 \omega_1^2 E_1 - \hat{\alpha} A (D_1 A) - 2i \hat{\alpha} \omega_1 E_2 \bar{A} - 2\hat{\beta} \bar{A} E_2 - 3\hat{\gamma} A^2 (E_4 + \bar{E}_4) - 6\hat{\gamma} A \bar{A} E_1 - 2i \hat{G} \omega_1^3 E_1 A \bar{A}}{-3\omega_1^2}$$

$$K_2 = \frac{[-6i \omega_1 (D_1 E_2) - 6i \hat{\xi}_1 \omega_1^2 E_2 - 2\hat{\beta} A E_1 - 3i \hat{\alpha} \omega_1 E_1 A - 6\hat{\gamma} A \bar{A} E_2 + 3\hat{G} \omega_1^2 A^2 (D_1 A) - 18i \hat{G} \omega_1^3 E_2 A \bar{A}]}{-8\omega_1^2}$$

$$K_3 = \frac{[-3\hat{\gamma} A^2 E_1 - 2\hat{\beta} A E_2 - 4i \hat{\alpha} \omega_1 A E_2 + 6i \hat{G} \omega_1^3 A^2 E_1]}{-15\omega_1^2}$$

$$K_4 = \frac{[-3\hat{\gamma} A^2 E_2 + 9i \hat{G} \omega_1^3 A^2 E_2]}{-24\omega_1^2}, K_5 = \frac{[-2i \Omega (D_1 E_3) - 2i \hat{\xi}_1 \omega_1 \Omega E_3 - 6\hat{\gamma} A \bar{A} E_3 - 6i \hat{G} \omega_1^2 \Omega E_3 A \bar{A}]}{\omega_1^2 - \Omega^2}$$

$$K_6 = \frac{[-i \Omega \hat{\alpha} A E_3 - i \hat{\alpha} \omega_1 A E_3 - 2\hat{\beta} E_3 A]}{\omega_1^2 - (\Omega + \omega_1)^2}, K_7 = \frac{[-i \Omega \hat{\alpha} \bar{A} E_3 + i \hat{\alpha} \omega_1 \bar{A} E_3 - 2\hat{\beta} E_3 \bar{A}]}{\omega_1^2 - (\Omega - \omega_1)^2}$$

$$K_8 = \frac{[3i \hat{G} \Omega E_3 \omega_1^2 A^2 - 3\hat{\gamma} A^2 E_3]}{\omega_1^2 - (\Omega + 2\omega_1)^2}, K_9 = \frac{[3i \hat{G} \Omega E_3 \omega_1^2 \bar{A}^2 - 3\hat{\gamma} \bar{A}^2 E_3]}{\omega_1^2 - (\Omega - 2\omega_1)^2}$$

$$K_{10} = \frac{6i \hat{G} \omega_1^3 E_1 \bar{A}^2 - \hat{\alpha} \bar{A} (D_1 \bar{A} + D_1 A) - 6\hat{\gamma} A \bar{A} (E_4 + \bar{E}_4) - 3\hat{\gamma} \bar{A}^2 E_1}{\omega_1^2}$$

$$r_1 = \xi_1 \omega_1 + \frac{9G \omega_1^2 a_{10}}{8} + \frac{F}{2\omega_1 a_{10}} \sin(\theta_{10})$$

$$r_2 = \frac{9G \omega_1 a_{10} F \sin(\theta_{10})}{16} + \frac{\xi_1 F}{2a_{10}} \sin(\theta_{10}) + \frac{F \sigma_1}{2\omega_1 a_{10}} \cos(\theta_{10}) - \frac{9\gamma a_{10} F \cos(\theta_{10})}{16\omega_1^2}$$

